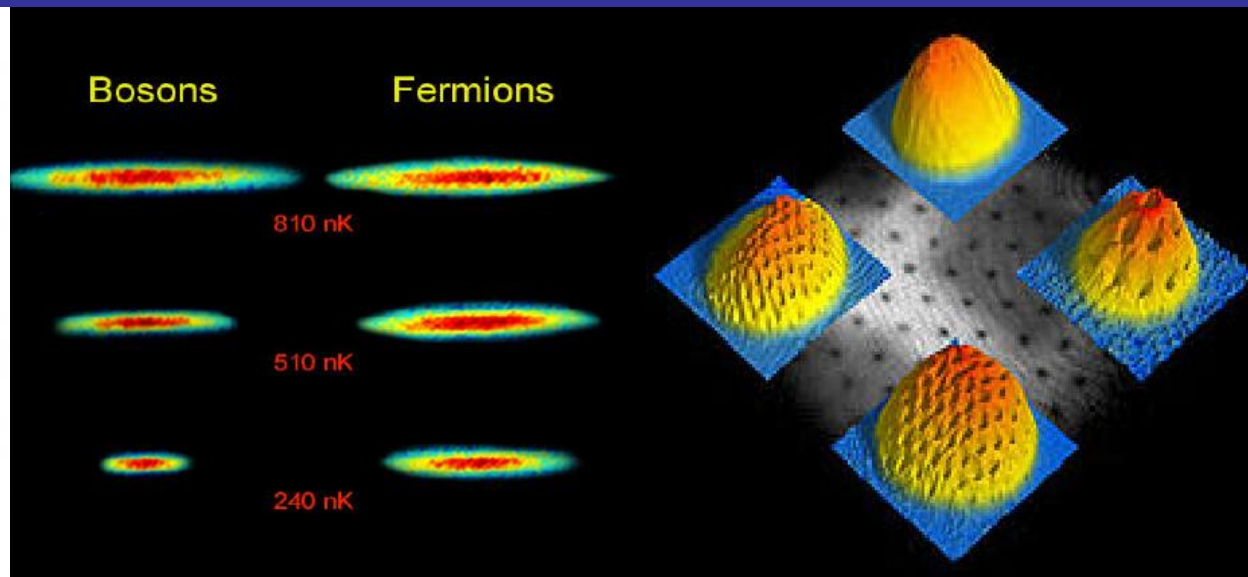
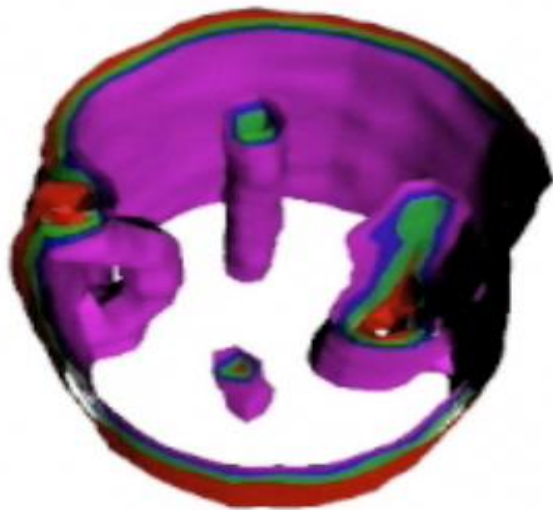


# *Equilibrium and nonequilibrium properties of unitary Fermi gas*



*Piotr Magierski*  
*Warsaw University of Technology*

# Collaborators:



Aurel Bulgac  
(U. Washington)



Kenneth J. Roche  
(PNNL)



Joaquin E. Drut  
(U. North Carolina)



Gabriel Wlazłowski  
(PW/ U. Washington)



Michael M. Forbes  
(INT)



Yongle Yu  
(Wuhan)



Yuan-Lung (Alan) Luo  
(U. Washington)

## What is a unitary gas?

A gas of interacting fermions is in the unitary regime if the average separation between particles is large compared to their size (range of interaction), but small compared to their scattering length.

$$n r_0^3 \ll 1 \quad n |a|^3 \gg 1$$

$n$  - particle density  
 $a$  - scattering length  
 $r_0$  - effective range

$$\text{i.e. } r_0 \rightarrow 0, a \rightarrow \pm\infty$$

**NONPERTURBATIVE  
REGIME**

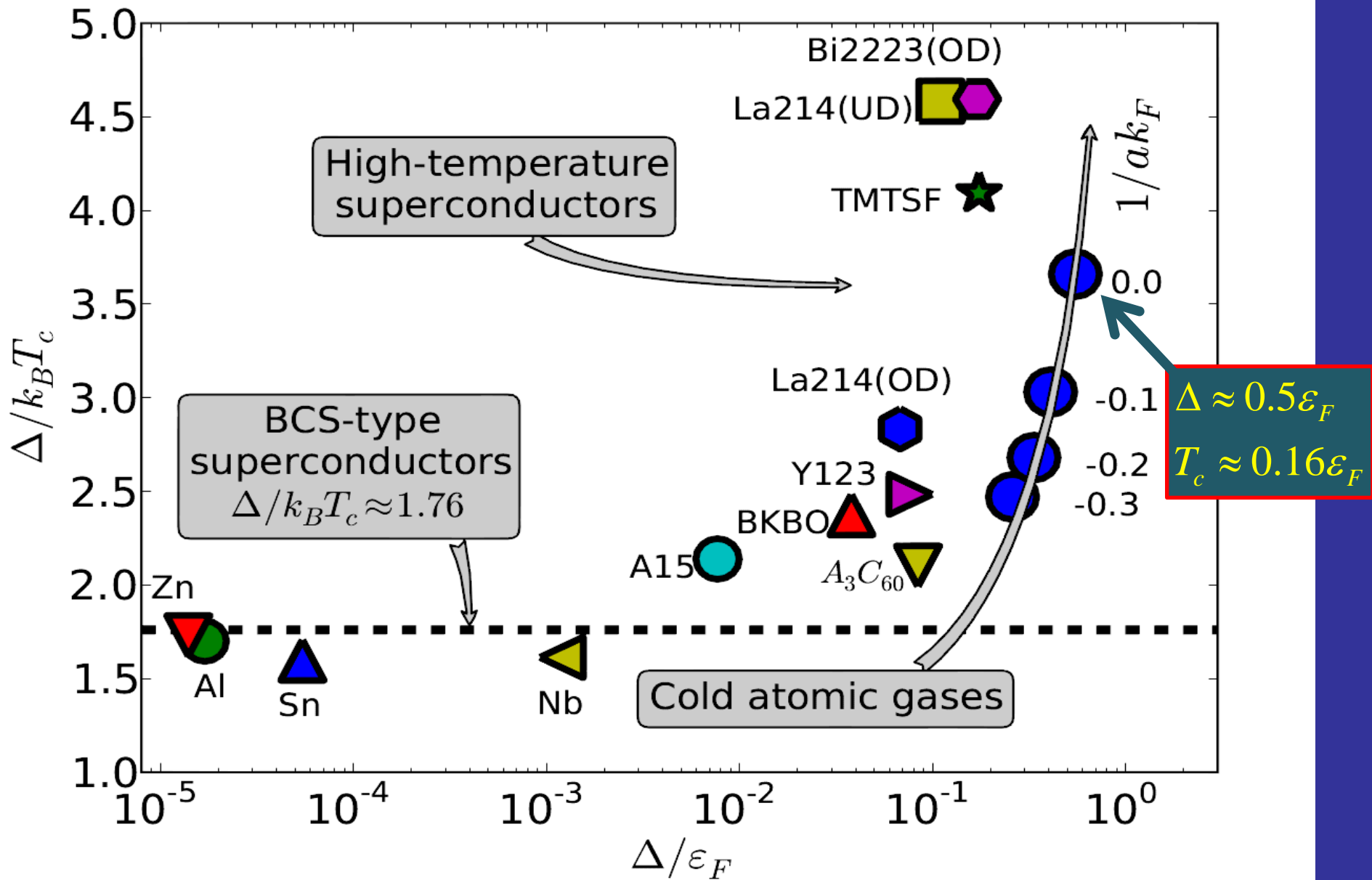
**System is dilute but  
strongly interacting!**

**Universality:**  $E(x) = \xi(x) E_{FG} \quad ; \quad x = \frac{T}{\epsilon_F}$

$$\xi(0) = 0.37(1) - \text{Exp. estimate}$$

$E_{FG}$  - Energy of noninteracting Fermi gas

# Cold atomic gases and high $T_c$ superconductors



# Expected phases of a two species dilute Fermi system BCS-BEC crossover

Characteristic temperature:  
 $T_c$  superfluid-normal  
phase transition

**Strong interaction  
UNITARY REGIME**

Characteristic temperatures:  
 $T_c$  superfluid-normal  
phase transition  
 $T^*$  break up of Bose molecule  
 $T^* > T_c$

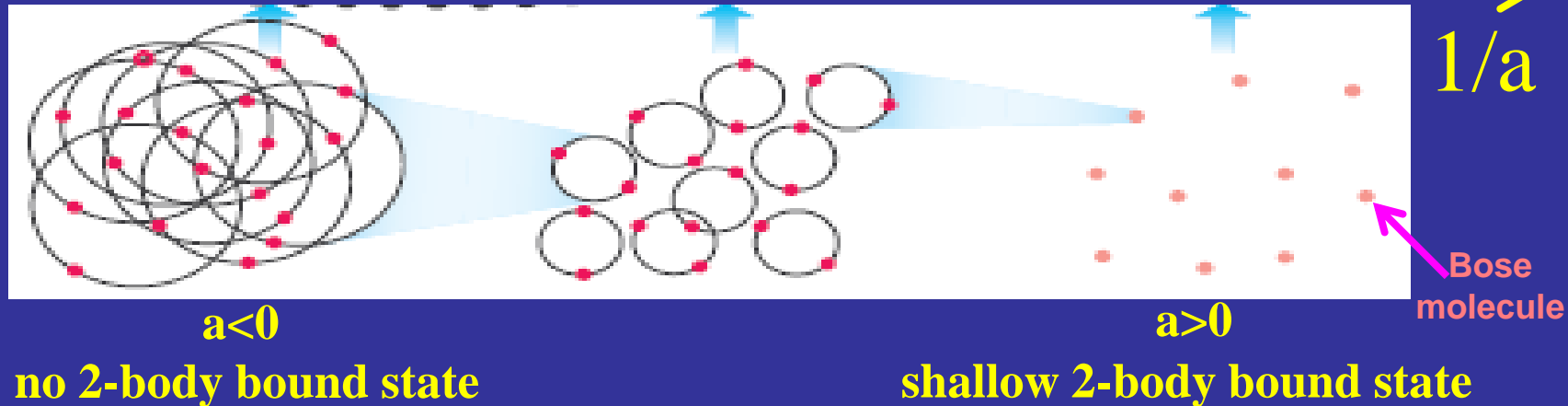
**weak interaction**

**BCS Superfluid**

**weak interactions**

**Molecular BEC and  
Atomic+Molecular  
Superfluids**

?

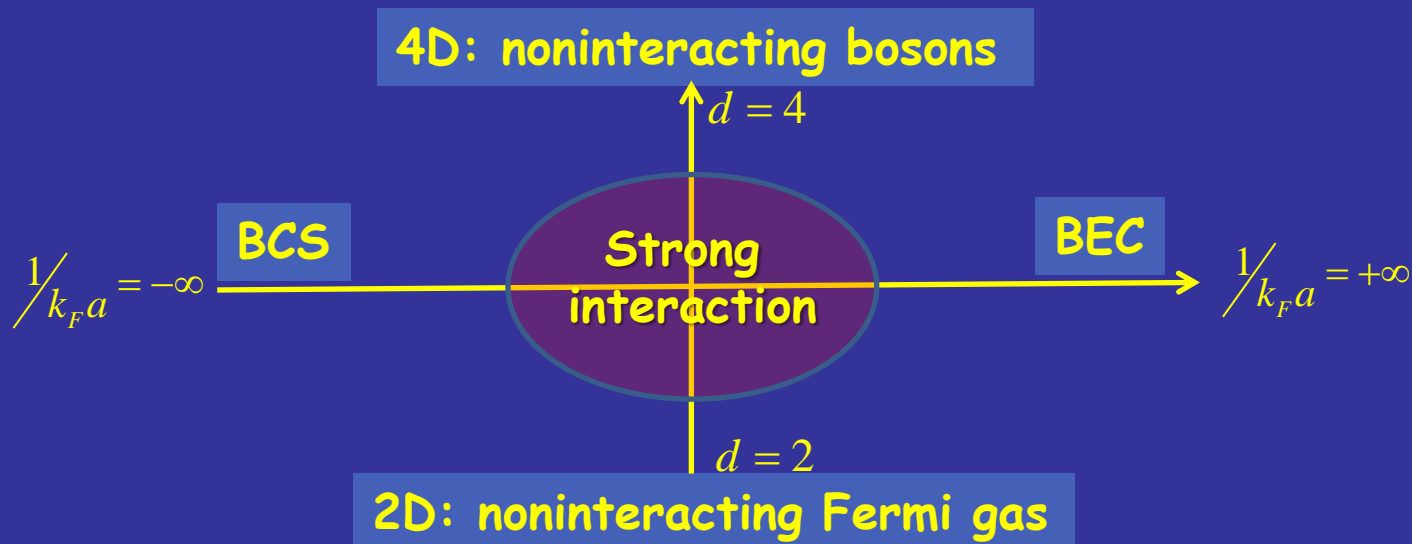


# Unitary limit in 2 and 4 dimensions:

$a \rightarrow \infty : R(r) \propto \frac{1}{r^{d-2}} + O(r^{4-d})$ , Two body wave function for  $r \rightarrow 0$ .

## Intuitive arguments:

- For  $d=4$   $\int R(r)^2 d^d r$  diverges at the origin
- For  $d=2$  the singularity of the wave function disappears = interaction also disappears.



**The only nontrivial case of unitary regime is in 3D**

# Effective Hamiltonian of an atom-atom system

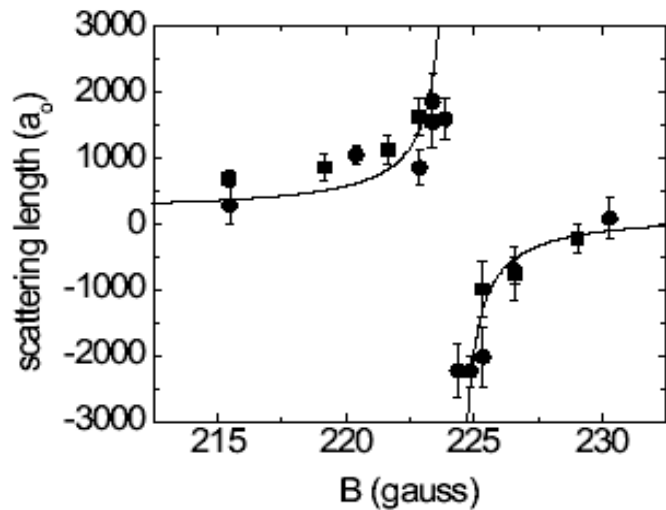
$$H = \frac{\vec{p}^2}{2\mu} + \sum_{i=1}^2 (V_i^{hf} + V_i^Z) + V_0(\vec{r})P_0 + V_1(\vec{r})P_1 + \dots$$

$$V^{hf} = \frac{a_{hf}}{\hbar^2} \vec{I} \cdot \vec{J}, \quad V_i - \text{Coulomb term}$$

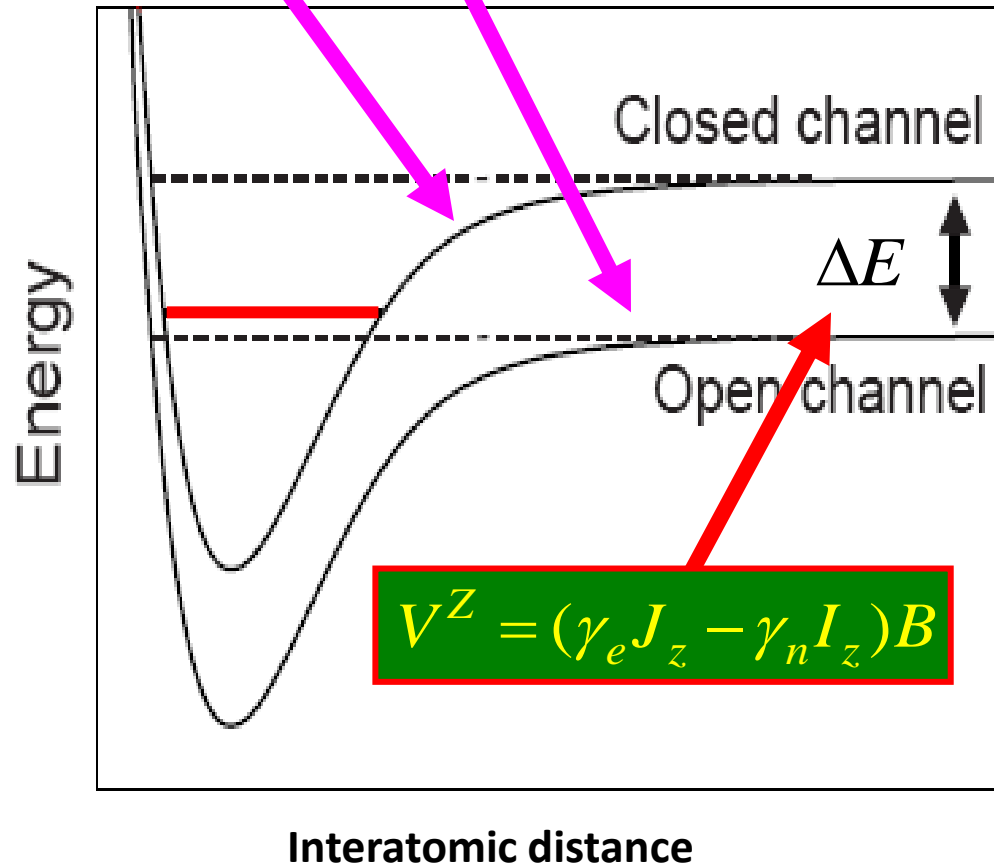
Tiesinga, Verhaar,  
Stoof, Phys. Rev.  
A47, 4114 (1993)

Channel coupling

Feshbach resonance



Regal and Jin, PRL 90, 230404 (2003)



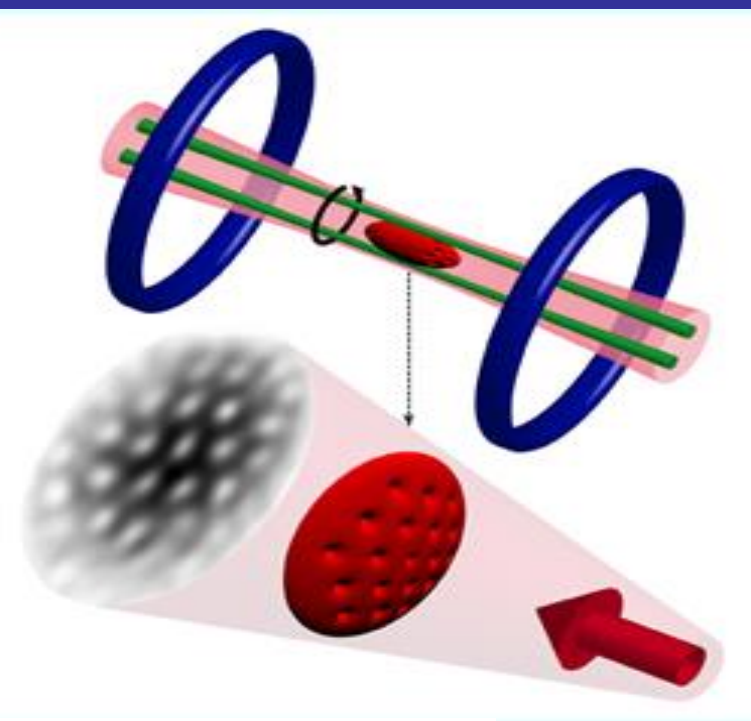
Interatomic distance

## Short (selective) history:

- ✓ In 1999 DeMarco and Jin created a degenerate atomic Fermi gas.
- ✓ In 2005 Zwierlein/Ketterle group observed quantum vortices which survived when passing from BEC to unitarity - evidence for superfluidity!

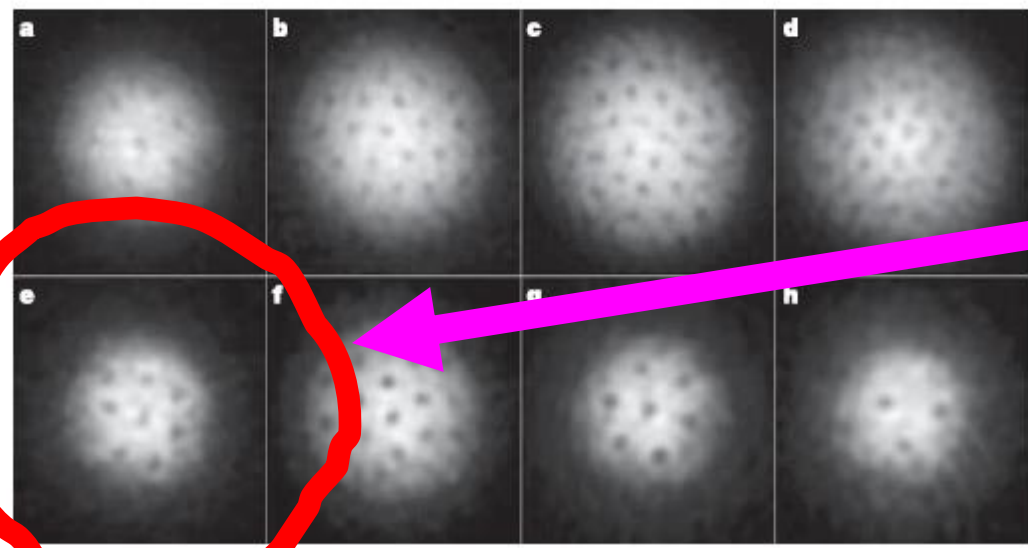
system of fermionic  ${}^6\text{Li}$  atoms

Feshbach resonance:  
 $B=834\text{G}$



BEC side:  
 $a > 0$

BCS side:  
 $a < 0$



UNITARY REGIME

Figure 2 | Vortices in a strongly interacting Fermionic atoms on the BEC- and the BCS-side of the Feshbach resonance. At the given field, the cloud of lithium atoms was stirred for 300 ms (a) or 500 ms (b–h) followed by an equilibration time of 500 ms. After 2 ms of ballistic expansion, the

magnetic field was ramped to 735 G for imaging (see Methods). The magnetic fields were 740 G (a), 766 G (b), 792 G (c), 843 G (f), 853 G (g) and 863 G (h). The field of view was  $880\ \mu\text{m} \times 880\ \mu\text{m}$ .

M.W. Zwierlein *et al.*,  
*Nature*, 435, 1047 (2005)



## Hamiltonian

$$\hat{H} = \hat{T} + \hat{V} = \int d^3 r \sum_{s=\uparrow\downarrow} \hat{\psi}_s^\dagger(\vec{r}) \left( -\frac{\hbar^2 \Delta}{2m} \right) \hat{\psi}_s(\vec{r}) - g \int d^3 r \hat{n}_\uparrow(\vec{r}) \hat{n}_\downarrow(\vec{r})$$

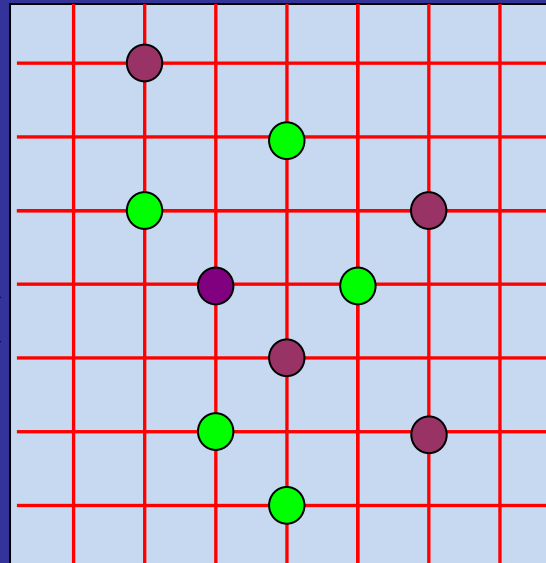
$$\hat{N} = \int d^3 r (\hat{n}_\uparrow(\vec{r}) + \hat{n}_\downarrow(\vec{r})); \quad \hat{n}_s(\vec{r}) = \hat{\psi}_s^\dagger(\vec{r}) \hat{\psi}_s(\vec{r})$$

## Path Integral Monte Carlo for fermions on 3D lattice

### Coordinate space

L-limit for the spatial correlations in the system

$$k_{cut} = \frac{\pi}{\Delta x}; \quad \Delta x$$



$$Volume = L^3$$

$$lattice\ spacing = \Delta x$$

● - Spin up fermion: ↑

● - Spin down fermion: ↓

External conditions:

$T$  - temperature

$\mu$  - chemical potential

Periodic boundary conditions imposed

# Basics of Auxiliary Field Monte Carlo (Path Integral MC)

$$\hat{H} = \hat{T} + \hat{V} = \int d^3r \sum_{s=\uparrow\downarrow} \hat{\psi}_s^\dagger(\vec{r}) \left( -\frac{\hbar^2 \Delta}{2m} \right) \hat{\psi}_s(\vec{r}) - g \int d^3r \hat{n}_\uparrow(\vec{r}) \hat{n}_\downarrow(\vec{r})$$

$$\hat{N} = \int d^3r (\hat{n}_\uparrow(\vec{r}) + \hat{n}_\downarrow(\vec{r})); \quad \hat{n}_s(\vec{r}) = \hat{\psi}_s^\dagger(\vec{r}) \hat{\psi}_s(\vec{r})$$

$$\frac{1}{g} = -\frac{m}{4\pi\hbar^2 a} + \frac{mk_{cut}}{2\pi^2\hbar^2}$$

Running coupling constant  $g$  defined by lattice

$$\frac{1}{g} = \frac{m}{2\pi\hbar^2 \Delta x} \quad - \text{UNITARY LIMIT}$$

$$\hat{U}(\{\sigma\}) = T_\tau \exp\left\{-\int_0^\beta d\tau [\hat{h}(\{\sigma\}) - \mu]\right\}; \quad \hat{h}(\{\sigma\}) - \text{one-body operator}$$

$$U(\{\sigma\})_{kl} = \langle \psi_k | \hat{U}(\{\sigma\}) | \psi_l \rangle; \quad |\psi_l\rangle - \text{single-particle wave function}$$

$$E(T) = \langle \hat{H} \rangle = \int \frac{D[\sigma(\vec{r}, \tau)] e^{-S[\sigma]}}{Z(T)} E[U(\{\sigma\})]$$

$E[U(\{\sigma\})]$  - energy associated with a given sigma field

$$\text{Tr} \hat{U}(\{\sigma\}) = \{\det[1 + \hat{U}_\uparrow(\sigma)]\}^2 = \exp[-S(\{\sigma\})] > 0 \quad - \text{No sign problem for spin symmetric system!}$$

## Details of calculations, improvements and problems

- Currently we can reach  $16^3$  lattice and perform calcs. down to  $x = 0.06$  ( $x$  – temperature in Fermi energy units) at the densities of the order of 0.03.
- Effective use of FFT(W) makes all imaginary time propagators diagonal (either in real space or momentum space) and there is no need to store large matrices.
- Update field configurations using the Metropolis importance sampling algorithm. QMC calculations can be split into two independent processes:
  - 1) sample generation (generation of sigma fields),
  - 2) calculations of observables.
- Change randomly at a fraction of all space and time sites the signs the auxiliary fields  $\sigma(\mathbf{r},\tau)$  so as to maintain a running average of the acceptance rate between 0.4 and 0.6 .
- At low temperatures use Singular Value Decomposition of the evolution operator  $U(\{\sigma\})$  to stabilize the numerics.
- MC correlation “time”  $\approx 200$  time steps at  $T \approx T_c$  for lattices  $10^3$  . Unfortunately when increasing the lattice size the correlation time also increases. One needs few thousands uncorrelated samples (we usually take about 10 000) to decrease the statistical error to the level of 1%.

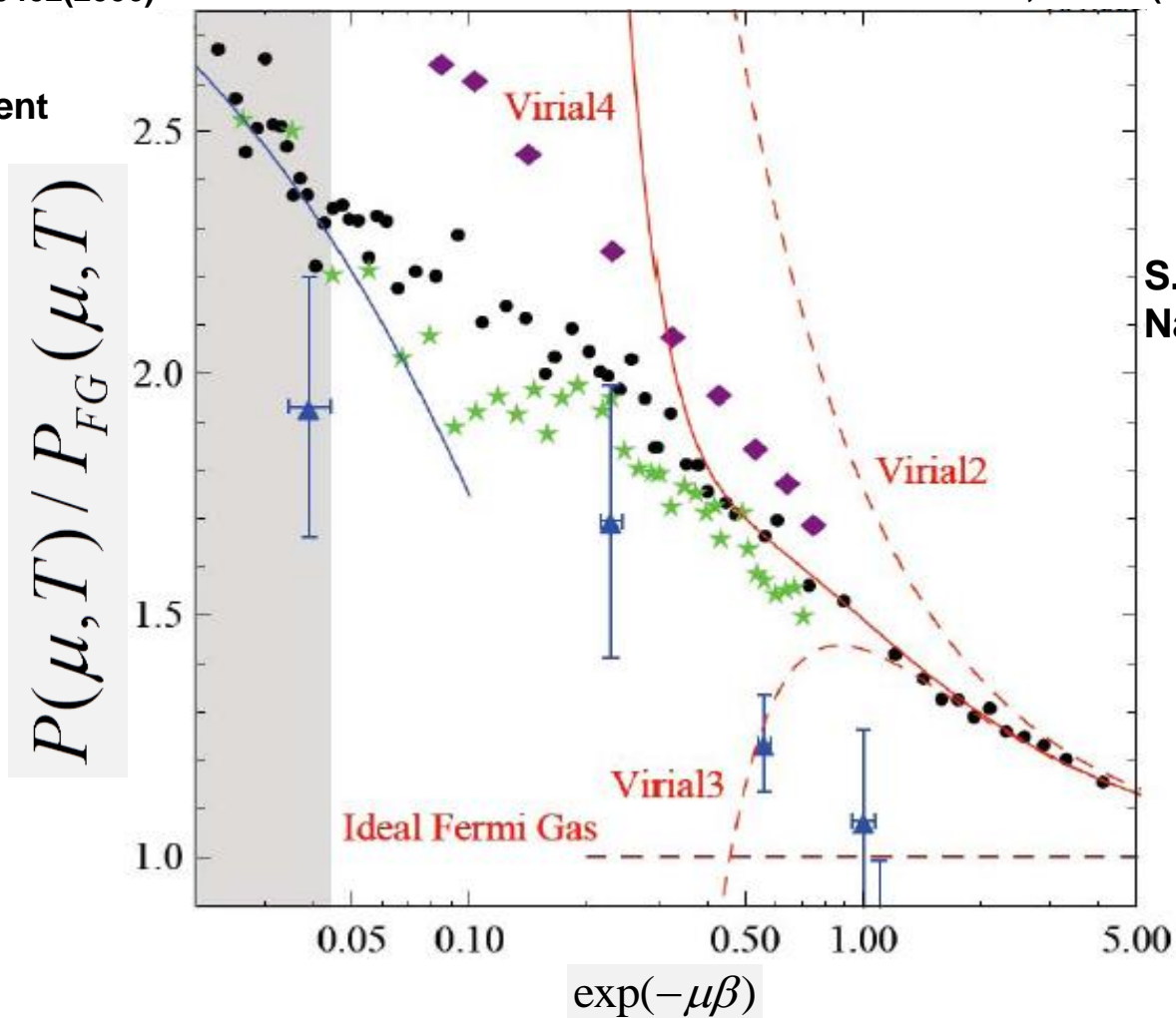
# Comparison with Many-Body Theories (1)

▲ Diagram. MC  
Burovski et al.  
PRL96, 160402(2006)

★ QMC  
Bulgac, Drut, Magierski,  
PRL99, 120401(2006)

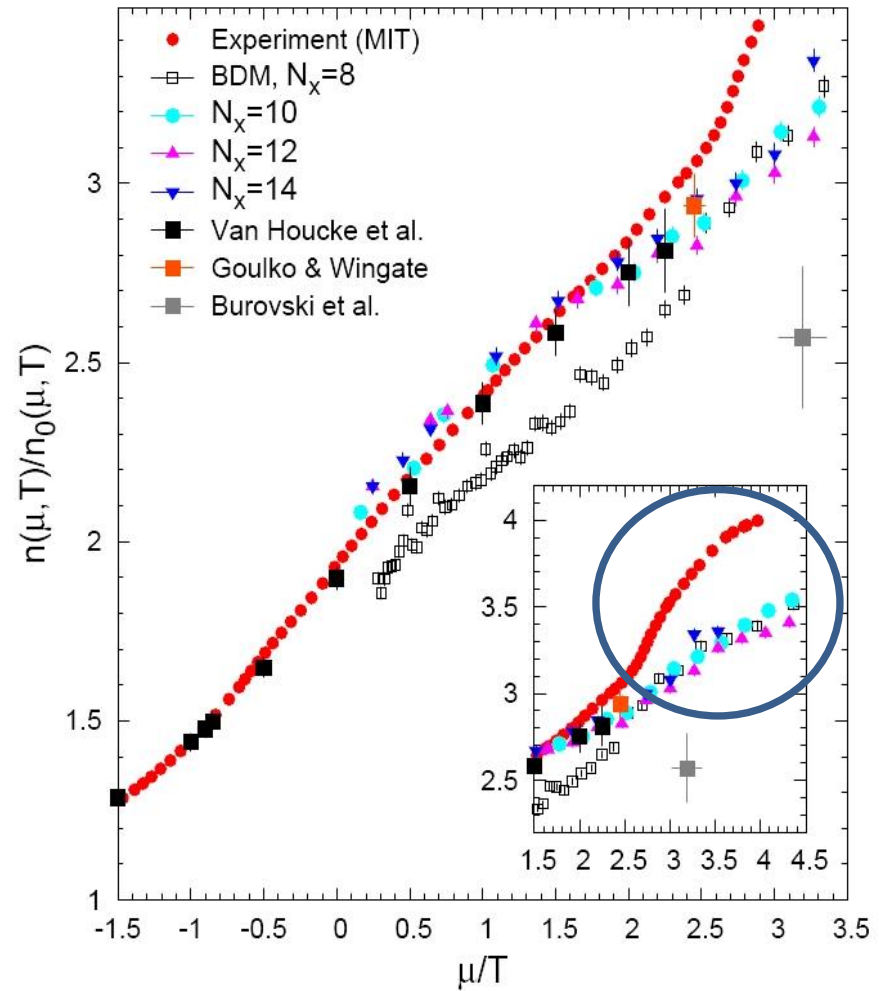
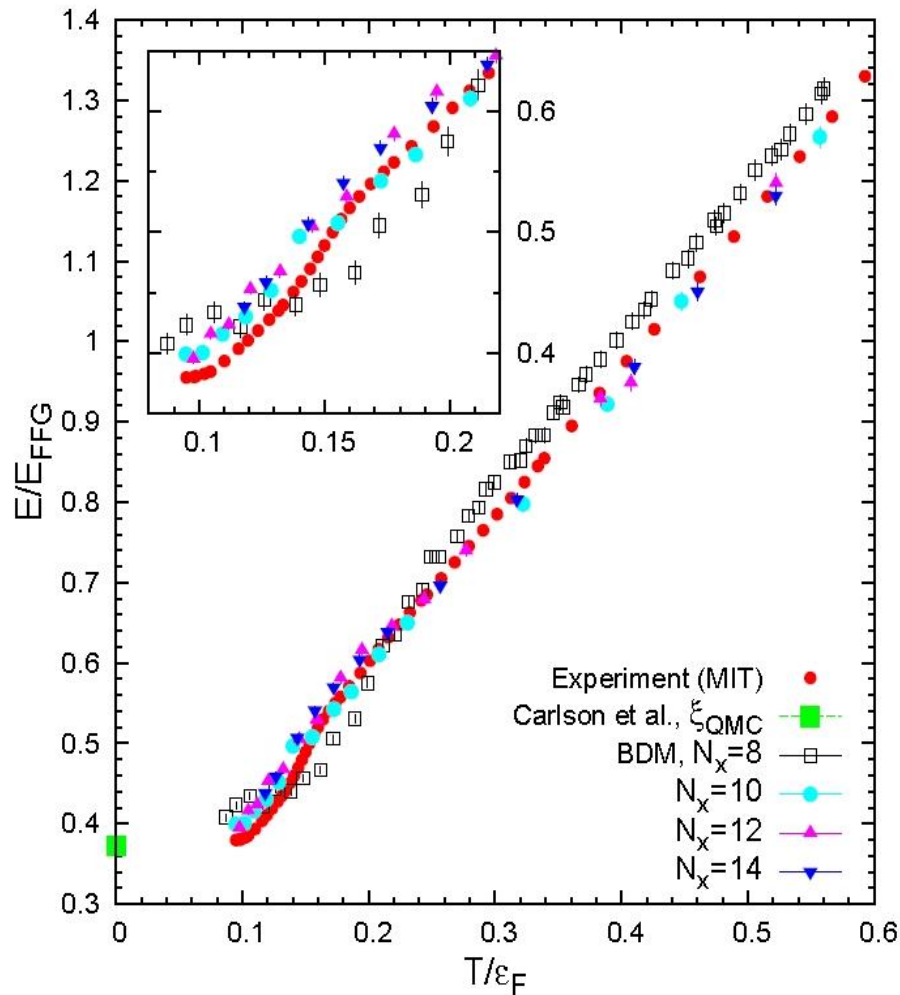
◆ Diagram. + analytic  
Hausmann et al.  
PRA75, 023610(2007)

● Experiment



S. Nascimbene et al.  
Nature 463, 1057 (2010)

# Equation of state of the unitary Fermi gas - current status



Experiment: M.J.H. Ku, A.T. Sommer, L.W. Cheuk, M.W. Zwierlein, Science 335, 563 (2012)

QMC (PIMC + Hybrid Monte Carlo): J.E. Drut, T. Lähde, G. Włazłowski, P. Magierski, Phys. Rev. A 85, 051601 (2012)

## Local density approximation (LDA) from QMC

Uniform  
system

$$\Omega = F - \lambda N = \frac{3}{5} \varphi(x) \varepsilon_F N - \lambda N$$

Nonuniform  
system

*(gradient  
corrections  
neglected)*

$$\Omega = \int d^3 r \left[ \frac{3}{5} \varepsilon_F(\vec{r}) \varphi(x(\vec{r})) + U(\vec{r}) - \lambda \right] n(\vec{r})$$

$$x(\vec{r}) = \frac{T}{\varepsilon_F(\vec{r})}; \quad \varepsilon_F(\vec{r}) = \frac{\hbar^2}{2m} \left[ 3\pi^2 n(\vec{r}) \right]^{2/3}$$

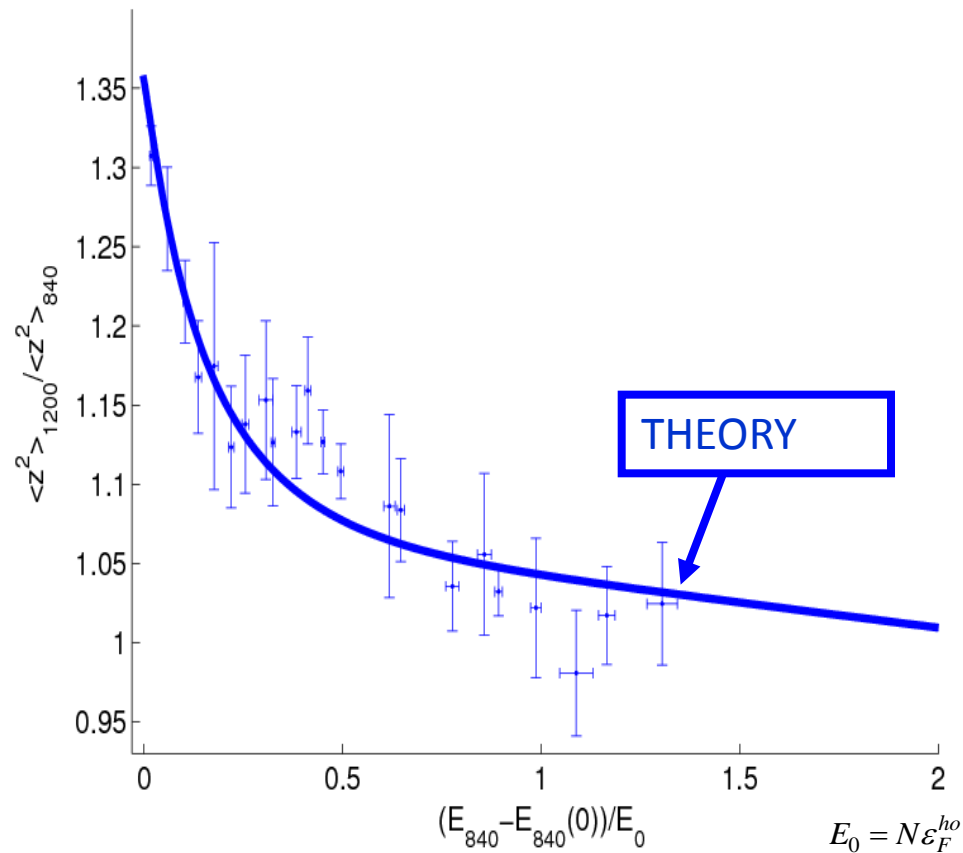
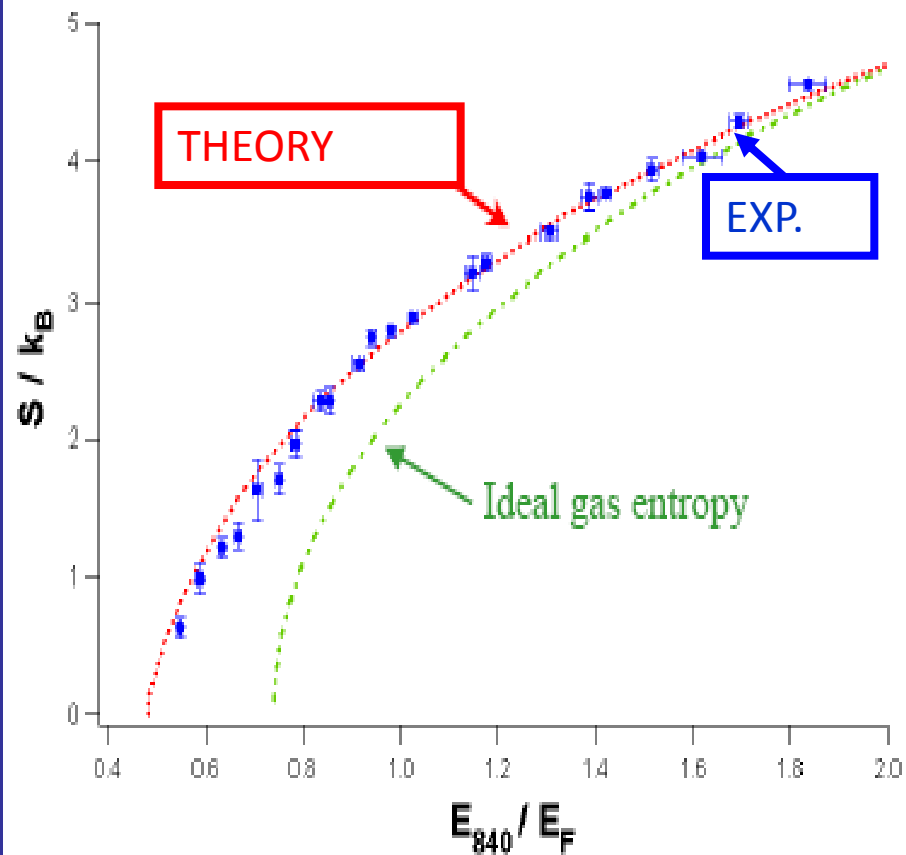
The overall chemical potential  $\lambda$  and the temperature  $T$  are constant throughout the system. The density profile will depend on the shape of the trap as dictated by:

$$\frac{\delta \Omega}{\delta n(\vec{r})} = \frac{\delta(F - \lambda N)}{\delta n(\vec{r})} = \mu(x(\vec{r})) + U(r) - \lambda = 0$$

Using as an input the Monte Carlo results for the uniform system and experimental data (trapping potential, number of particles), we determine the density profiles.

## Comparison with experiment

John Thomas' group at Duke University,  
L.Luo, et al. Phys. Rev. Lett. 98, 080402, (2007)



Entropy as a function of energy (relative to the ground state) for the unitary Fermi gas in the harmonic trap.

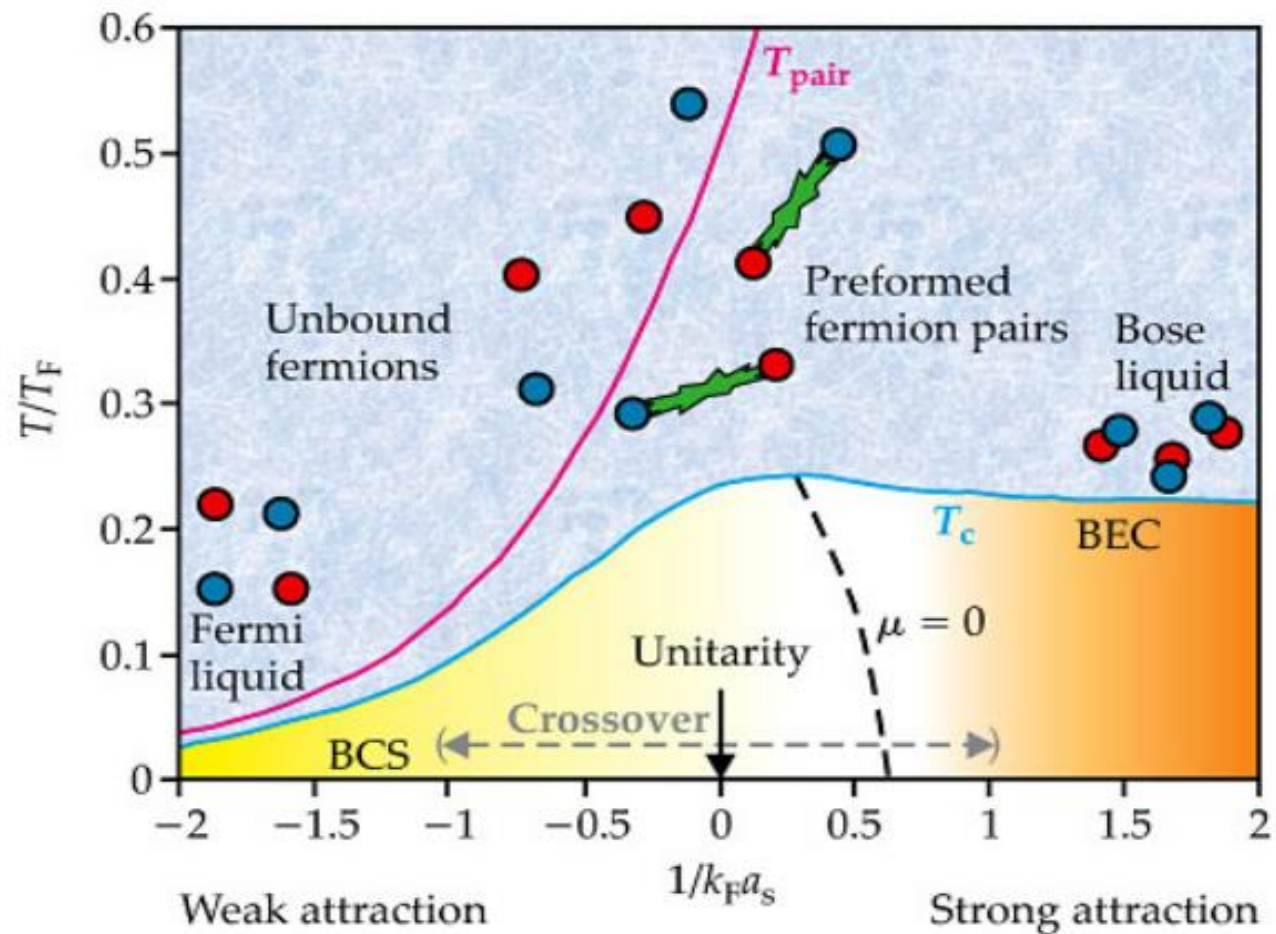
Ratio of the mean square cloud size at  $B=1200G$  to its value at unitarity ( $B=840G$ ) as a function of the energy. Experimental data are denoted by point with error bars.

$$B = 1200G \Rightarrow 1/k_F a \approx -0.75$$

Theory:

Bulgac, Drut, and Magierski  
PRL 99, 120401 (2007)

From Sa de Melo,  
Physics Today (2008)



Pairing pseudogap: suppression of low-energy spectral weight function due to incoherent pairing in the normal state ( $T > T_c$ )

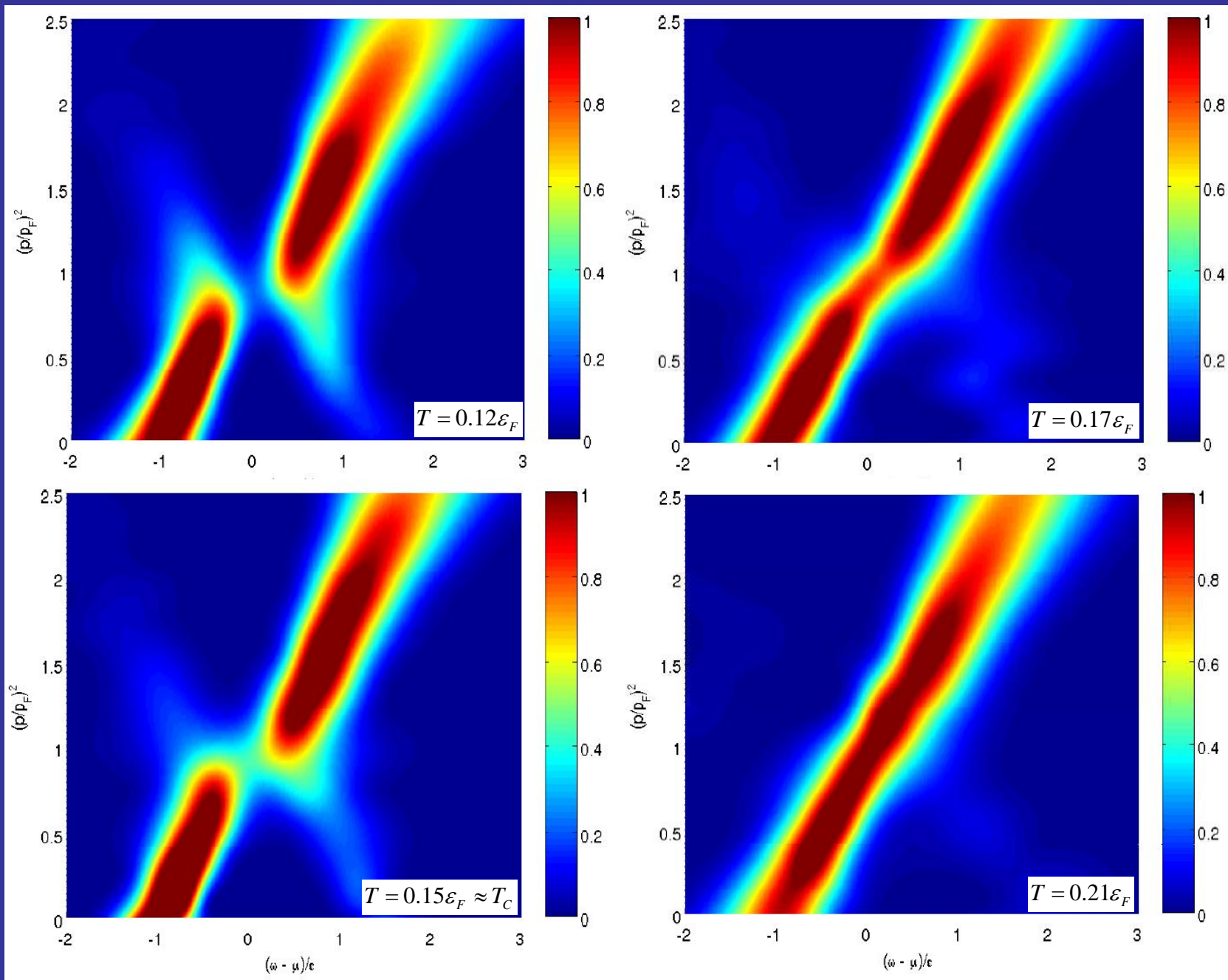
Important issue related to pairing pseudogap:

- Are there sharp gapless quasiparticles in a normal Fermi liquid  
YES: Landau's Fermi liquid theory;  
NO: breakdown of Fermi liquid paradigm

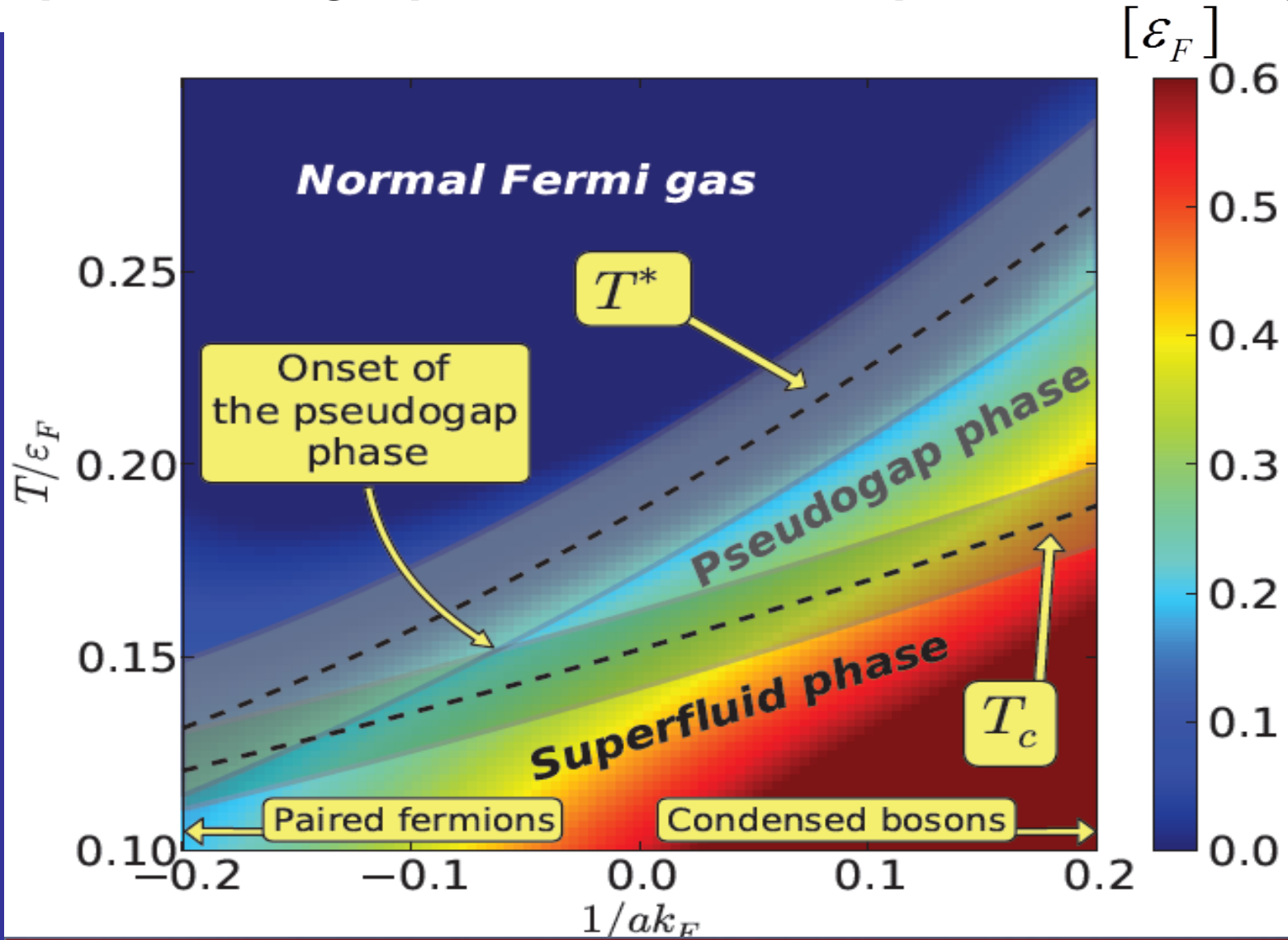


# Spectral weight function at unitarity:

$$(k_F a)^{-1} = 0$$

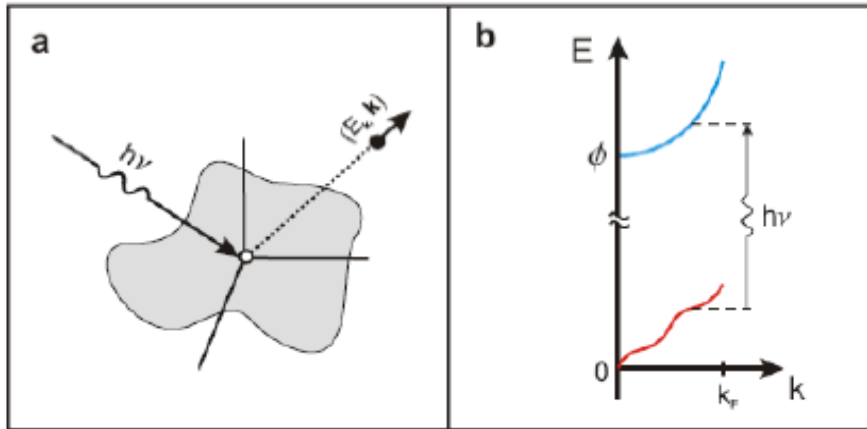


# Gap in the single particle fermionic spectrum - theory

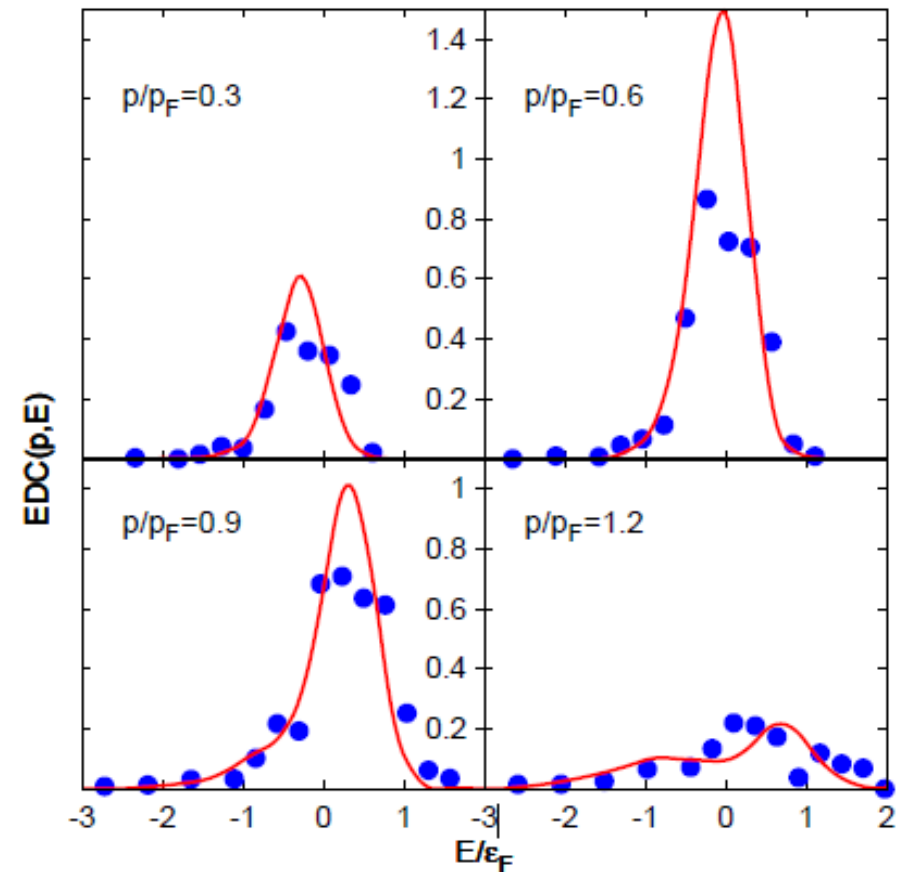


**Ab initio result: The onset of pseudogap phase at  $1/ak_F \approx -0.05$ .**

# RF spectroscopy in ultracold atomic gases



$$\text{EDC}(p, E, T) = C p^2 \int_0^\infty dr r^2 \frac{1}{\varepsilon_F(r)} A\left[\frac{p}{p_F(r)}, \frac{E - \mu(r)}{\varepsilon_F(r)}, \frac{T}{\varepsilon_F(r)}\right] f(E - \mu(r)),$$



$$-E_s + h\nu = \frac{\hbar^2 k^2}{2m} + \phi$$

$$E(N) = E(N-1) + E_s$$

Stewart, Gaebler, Jin, Using photoemission spectroscopy to probe a strongly interacting Fermi gas, *Nature*, 454, 744 (2008)

Experiment (blue dots): D. Jin's group Gaebler et al. *Nature Physics* 6, 569(2010)  
Theory (red line): Magierski, Wlazłowski, Bulgac, *Phys.Rev.Lett.*107,145304(2011)

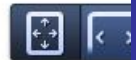
# Viscosity in strongly correlated quantum systems:

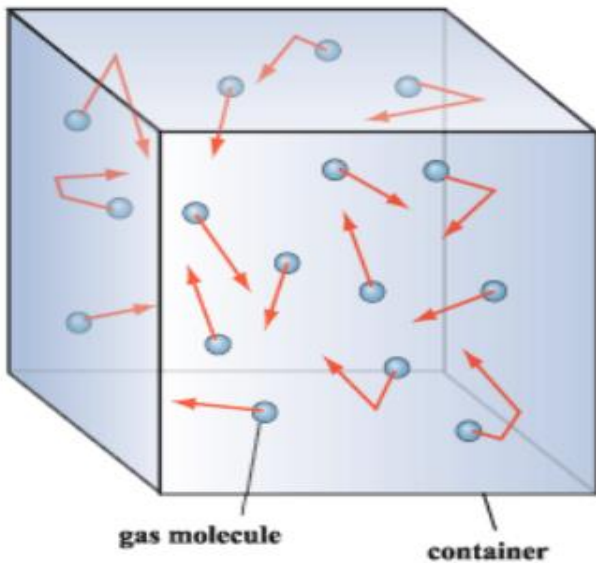


WWW.FOTOSHOP.COM FC00-6654 Foodcollection  
Pouring water out of glass into glass

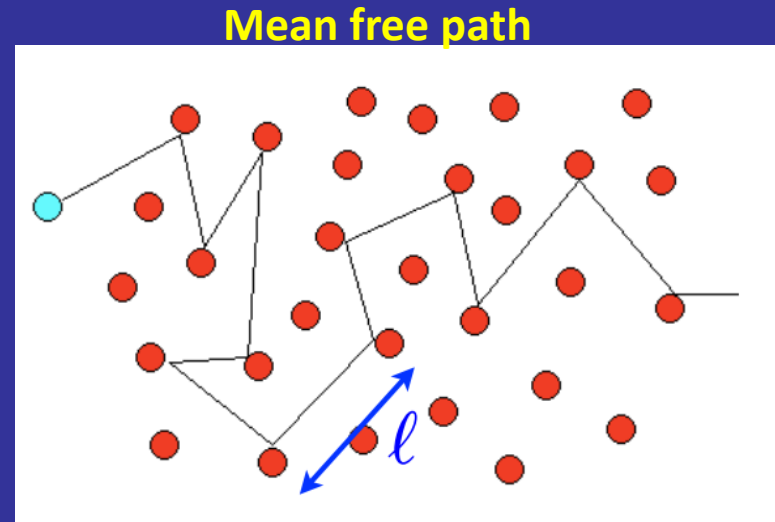


Water and honey flow with different rates:  
different viscosity





In the light of the kinetic theory of gases molecules are moving mostly along straight lines and occasionally bump onto each other.



This leads to the Maxwell's formula for viscosity (1860):

$$\eta \sim \rho v l = \text{mass density} \times \text{velocity} \times \text{mean free path}$$

### Consequences:

- Non interacting gas is a pathological example of the system with an infinite viscosity
- Strongly interacting system can have low viscosity since the mean free path is short **but...**

...but when the system is strongly correlated then the kinetic theory fails!

However:

If we blindly use this formula we may notice that the Heisenberg uncertainty principle would give the following relation:

$$\frac{\eta}{\rho} \sim \bar{p}l \geq \hbar$$

$\bar{p}$  - average momentum

*For any physical fluid:*

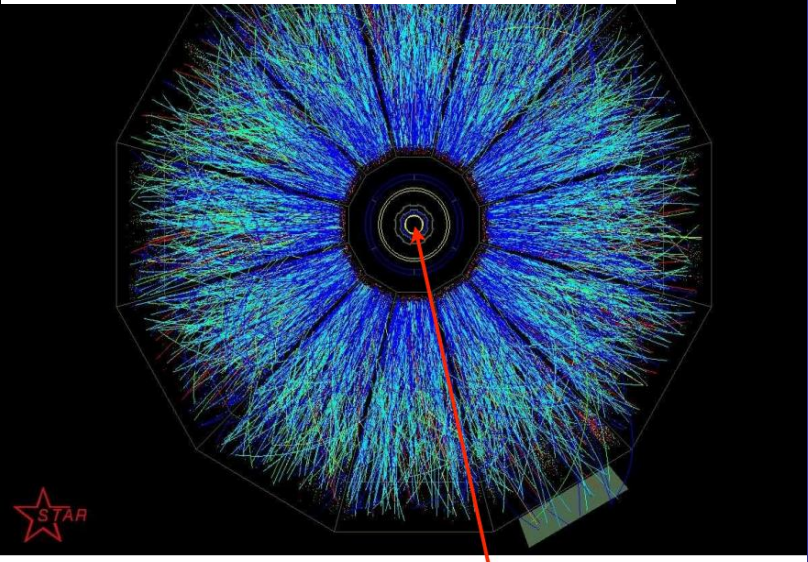
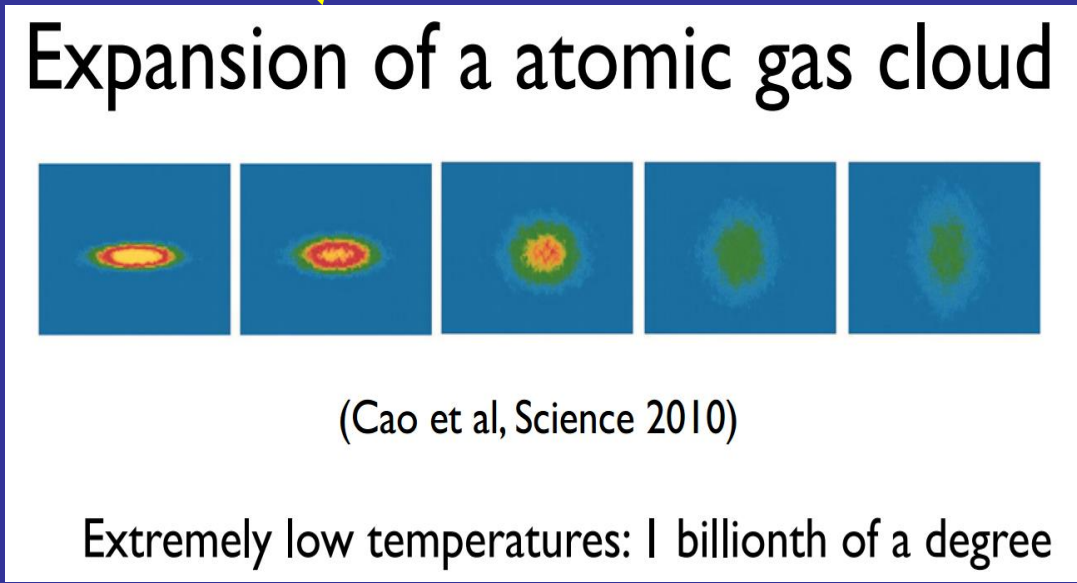
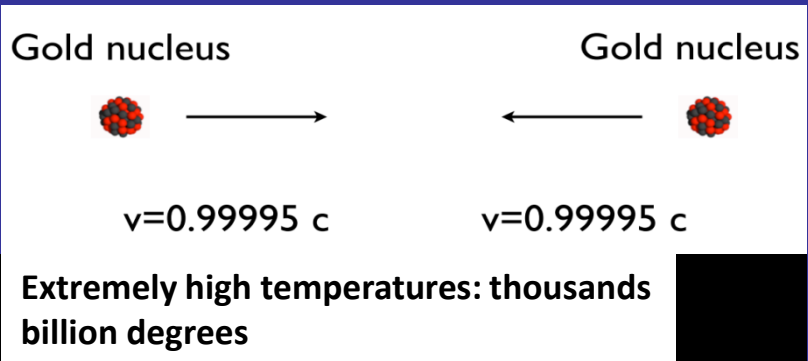
$$\frac{\eta}{S} \geq \frac{\hbar}{4\pi k_B}$$

**KSS conjecture**

Kovtun, Son, Starinets, Phys.Rev.Lett. 94, 111601, (2005)  
from AdS/CFT correspondence

Perfect fluid  $\frac{\eta}{S} = \frac{\hbar}{4\pi k_B}$  - strongly interacting quantum system = No well defined quasiparticles

**Candidates: quark gluon plasma, atomic gas**



a very dense droplet of matter in the beginning

Despite of energy scales differing by many orders of magnitude, expansion of both system is pretty much similar and in particular exhibits the so-called elliptic flow.

## Shear viscosity

$$\eta(\omega) = \pi \rho_{xyxy}(q=0, \omega) / \omega$$

$$G_{xyxy}(q, \tau) = \int d^3 r \langle \hat{\Pi}_{xy}(r, \tau) \hat{\Pi}_{xy}(0, 0) \rangle e^{iqr}$$

$$G_{xyxy}(q, \tau) = \int_0^{\infty} \rho_{xyxy}(q, \omega) \frac{\cosh[\omega(\tau - \beta/2)]}{\sinh[\omega\beta/2]} d\omega$$

$$i \left[ \hat{j}_k(r), \hat{H} \right] = \partial_l \hat{\Pi}_{kl}(r)$$

### Additional symmetries and sum rules:

$$G(\tau) = G(\beta - \tau)$$

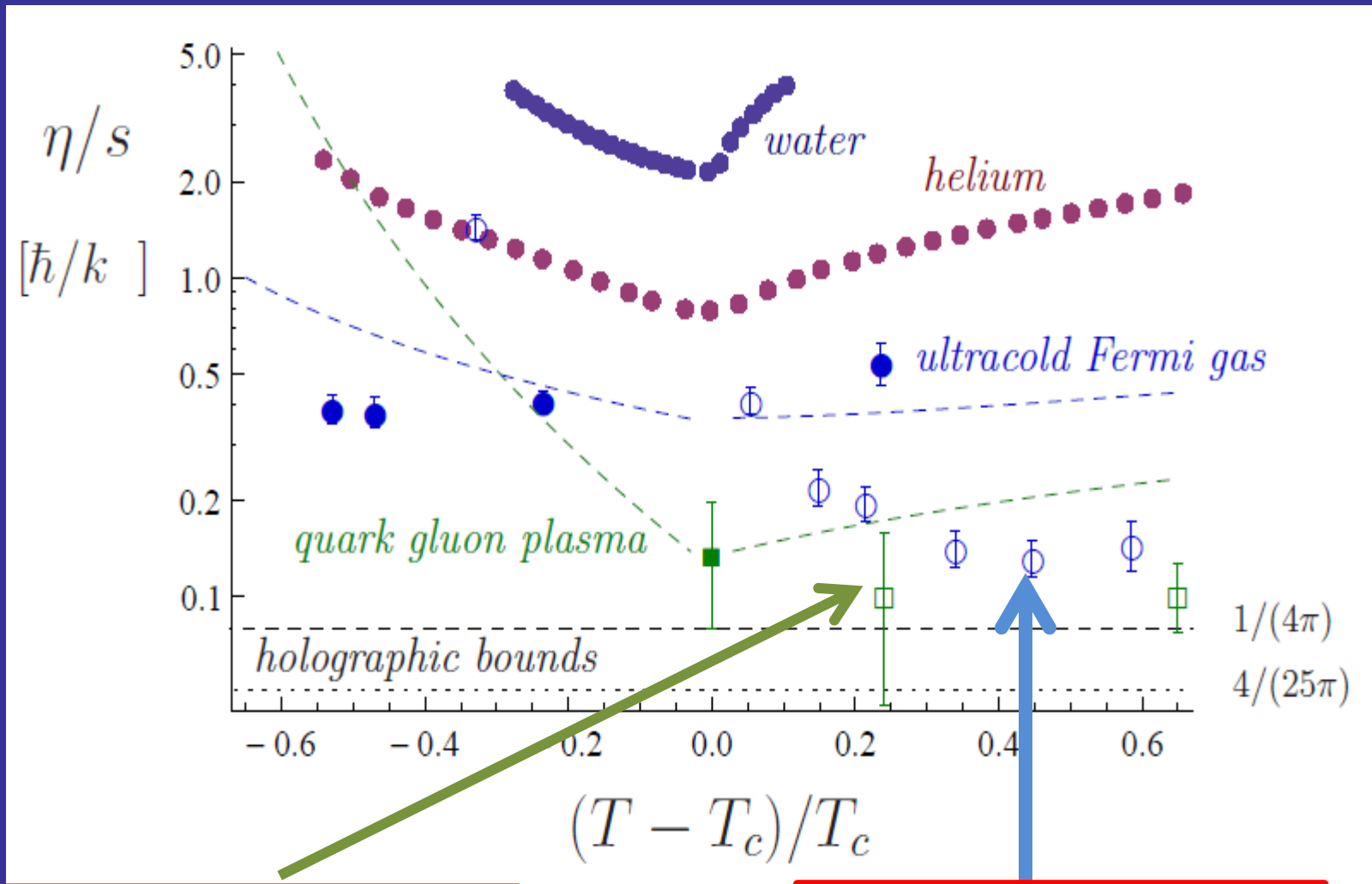
$$\frac{1}{\pi} \int_0^{\infty} d\omega \left[ \eta(\omega) - \frac{C}{15\pi\sqrt{m\omega}} \right] = \frac{\varepsilon}{3}, \quad \varepsilon - \text{energy density}$$

$$\eta(\omega \rightarrow \infty) \simeq \frac{C}{15\pi\sqrt{m\omega}}.$$



# Shear viscosity to entropy ratio – experiment vs. theory

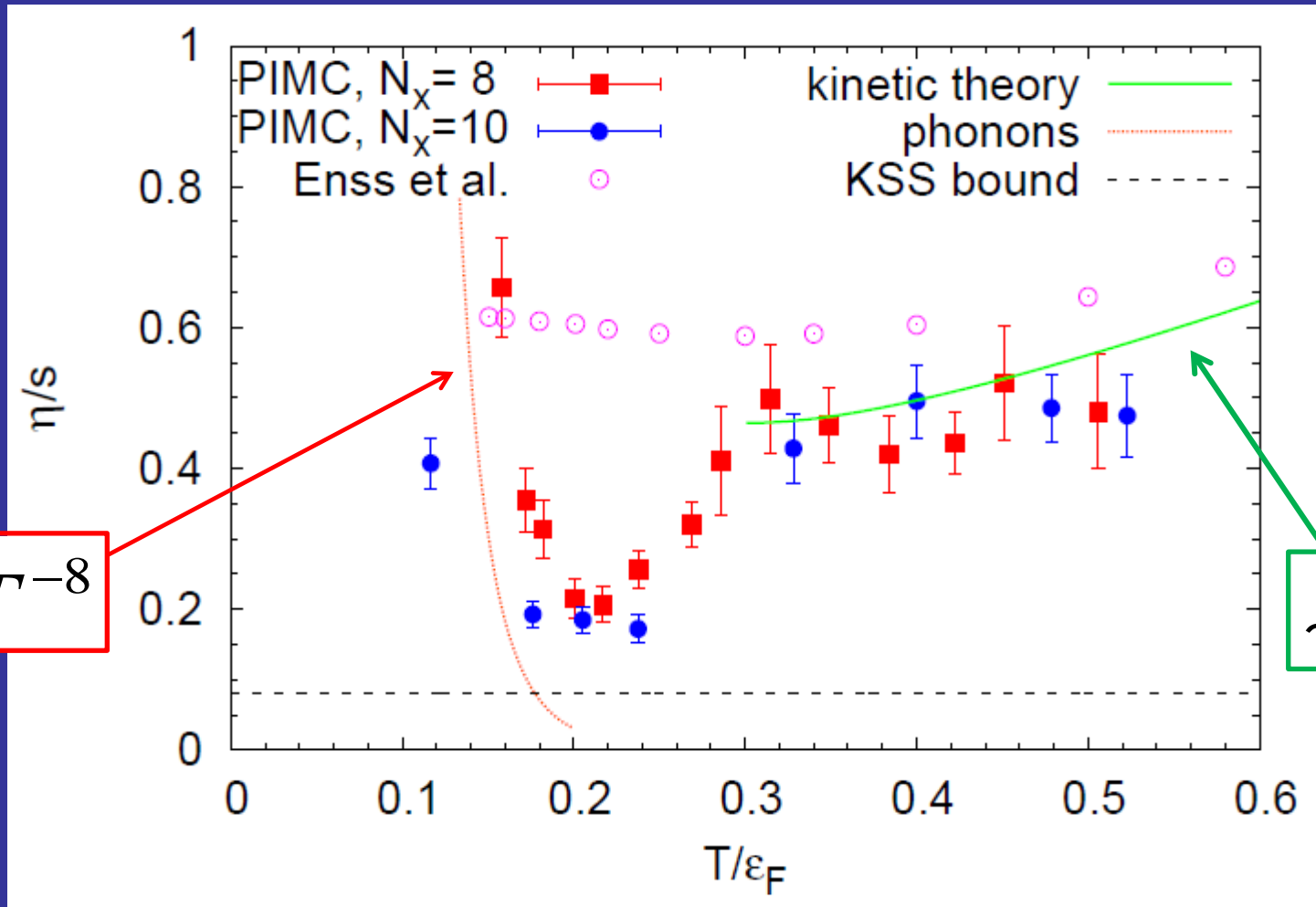
(from *A. Adams et al.* New Journal of Physics, "Focus on Strongly Correlated Quantum Fluids: from Ultracold Quantum Gases to QCD Plasmas,, arXiv:1205.5180)



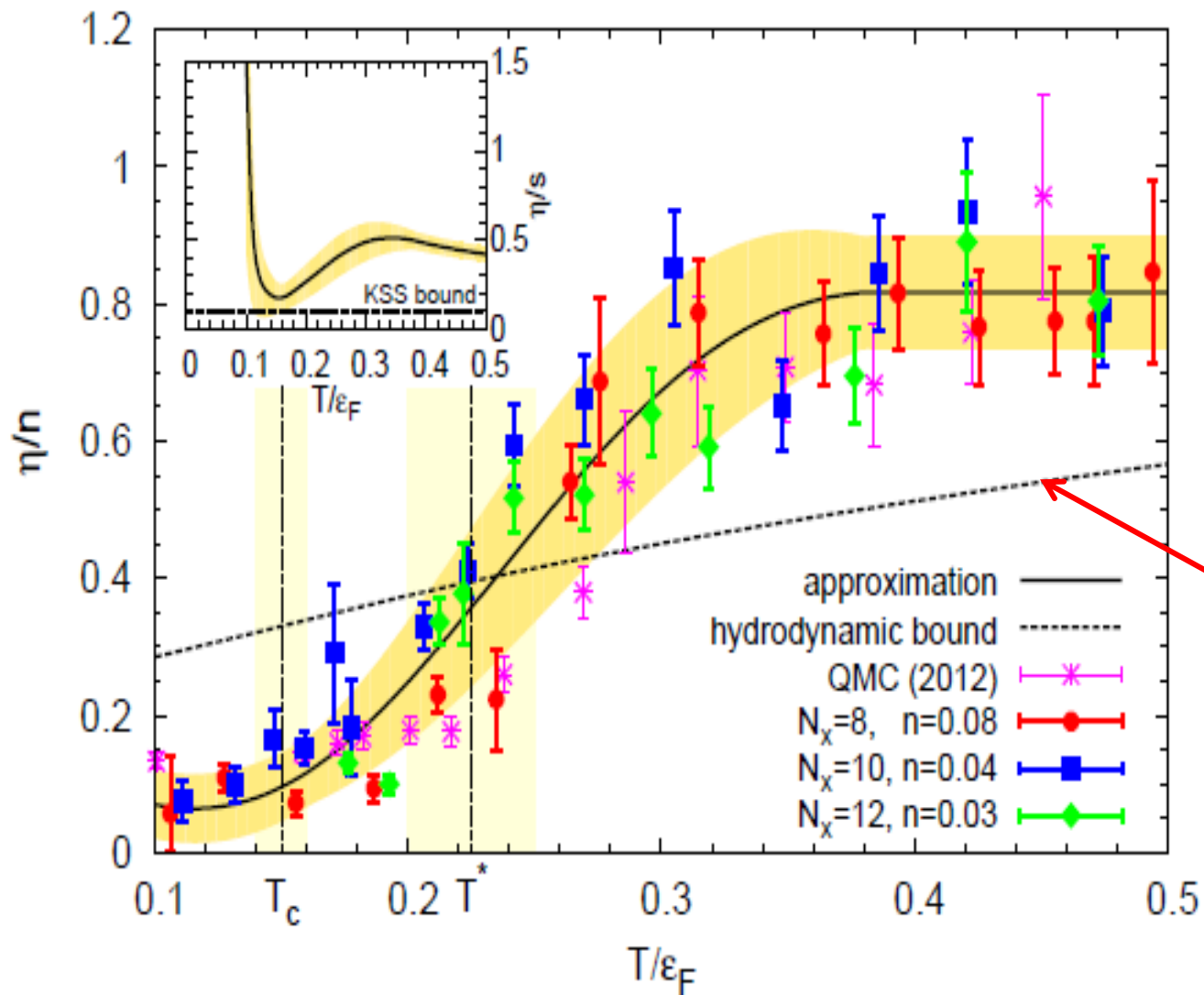
Lattice QCD ( SU(3) gluodynamics ):  
H.B. Meyer, Phys. Rev. D 76, 101701 (2007)

QMC calculations for UFG:  
G. Wlazłowski, P. Magierski, J.E. Drut,  
Phys. Rev. Lett. 109, 020406 (2012)

# Shear viscosity to entropy density ratio



# Shear viscosity per unit density as a function of temperature



C. Chafin, T. Schafer,  
PRA87,023629(2013)  
P.Romatschke, R.E. Young,  
arXiv:1209.1604

# Spin susceptibility and spin drag rate

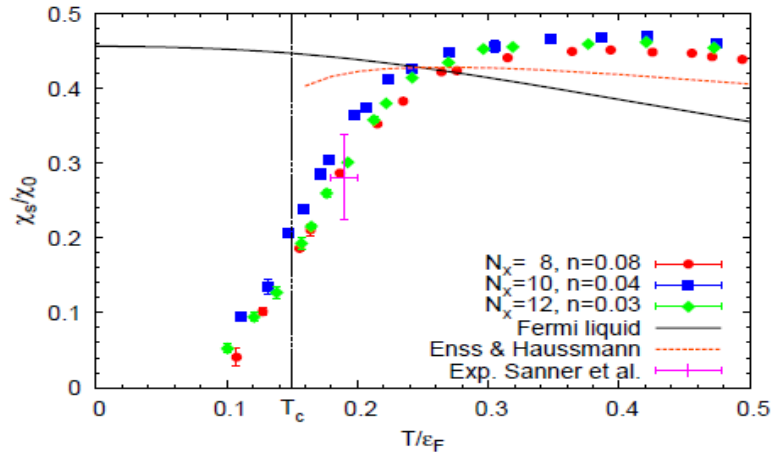


FIG. 2: (Color online) The static spin susceptibility as a function of temperature for an  $8^3$  lattice solid (red) circles,  $10^3$  lattice (blue) squares and  $12^3$  lattice (green) diamonds. Vertical black dotted line indicates the critical temperature of superfluid to normal phase transition  $T_c = 0.15 \varepsilon_F$ . For comparison Fermi liquid theory prediction and recent results of the  $T$ -matrix theory produced by Enss and Haussmann [25] are plotted with solid and dashed (brown) lines, respectively. The experimental data point from Ref. [15] is also shown.

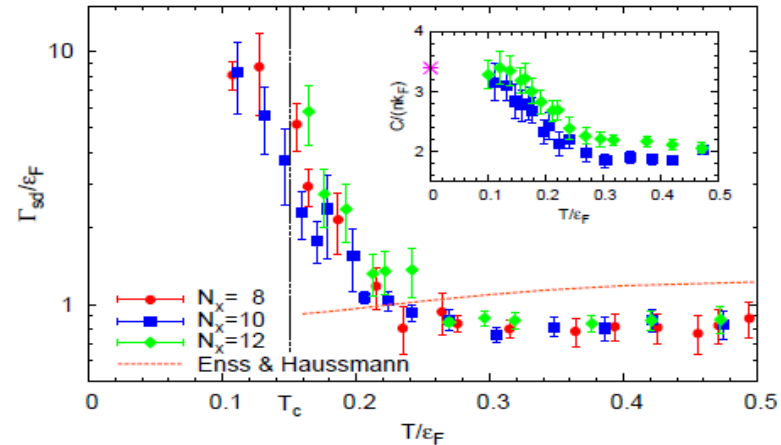


FIG. 3: (Color online) The spin drag rate  $\Gamma_{sd} = n/\sigma_s$  in units of Fermi energy as a function of temperature for an  $8^3$  lattice solid (red) circles,  $10^3$  lattice (blue) squares and  $12^3$  lattice (green) diamonds. Vertical black dotted line locates the critical temperature of superfluid to normal phase transition. Results of the  $T$ -matrix theory are plotted by dashed (brown) line [25]. The inset shows extracted value of the contact density as function of the temperature. The (purple) asterisk shows the contact density from the QMC calculations of Ref. [29] at  $T = 0$ .

$$\Gamma = \frac{n}{\sigma_s} \quad \text{- spin drag rate}$$

$$\sigma_s(\omega) = \pi \rho_s(q=0, \omega) / \omega \quad \text{- spin conductivity}$$

$$G_s(q, \tau) = \frac{1}{V} \left\langle \left( \hat{j}_{q\uparrow}^z(\tau) - \hat{j}_{q\downarrow}^z(\tau) \right) \left( \hat{j}_{-q\uparrow}^z(0) - \hat{j}_{-q\downarrow}^z(0) \right) \right\rangle$$

$$G_s(q, \tau) = \int_0^\infty \rho_s(q, \omega) \frac{\cosh[\omega(\tau - \beta/2)]}{\sinh[\omega\beta/2]} d\omega$$

# Formalism for Time Dependent Phenomena: TDSLDA

A.K. Rajagopal and J. Callaway, Phys. Rev. B 7, 1912 (1973)  
 V. Peuckert, J. Phys. C 11, 4945 (1978)  
 E. Runge and E.K.U. Gross, Phys. Rev. Lett. 52, 997 (1984)

$$i\hbar \frac{\partial}{\partial t} \begin{pmatrix} u_{k\uparrow}(\mathbf{r}, t) \\ u_{k\downarrow}(\mathbf{r}, t) \\ v_{k\uparrow}(\mathbf{r}, t) \\ v_{k\downarrow}(\mathbf{r}, t) \end{pmatrix} = \begin{pmatrix} h_{\uparrow,\uparrow}(\mathbf{r}, t) & h_{\uparrow,\downarrow}(\mathbf{r}, t) & 0 & \Delta(\mathbf{r}, t) \\ h_{\downarrow,\uparrow}(\mathbf{r}, t) & h_{\downarrow,\downarrow}(\mathbf{r}, t) & -\Delta(\mathbf{r}, t) & 0 \\ 0 & -\Delta^*(\mathbf{r}, t) & -h_{\uparrow,\uparrow}^*(\mathbf{r}, t) & -h_{\uparrow,\downarrow}^*(\mathbf{r}, t) \\ \Delta^*(\mathbf{r}, t) & 0 & -h_{\uparrow,\downarrow}^*(\mathbf{r}, t) & -h_{\downarrow,\downarrow}^*(\mathbf{r}, t) \end{pmatrix} \begin{pmatrix} u_{k\uparrow}(\mathbf{r}, t) \\ u_{k\downarrow}(\mathbf{r}, t) \\ v_{k\uparrow}(\mathbf{r}, t) \\ v_{k\downarrow}(\mathbf{r}, t) \end{pmatrix}$$

Density functional contains normal densities, anomalous density (pairing) and currents:

$$E(t) = \int d^3r \left[ \varepsilon(n(\vec{r}, t), \tau(\vec{r}, t), \nu(\vec{r}, t), \underline{\vec{j}}(\vec{r}, t)) + V_{ext}(\vec{r}, t)n(\vec{r}, t) + \dots \right]$$

Density  
functional for  
unitary Fermi  
gas

Nuclear energy  
functional: SLy4,  
SkP, SkM\*, ...

Both codes: SLDA and TDSLDA are formulated on the 3D lattice without any symmetry restrictions.

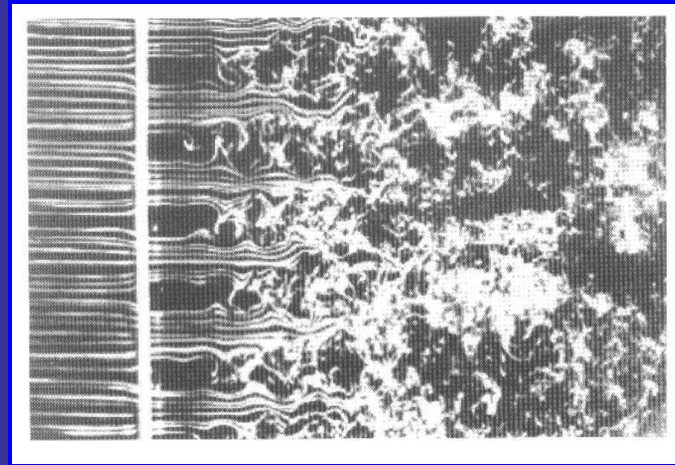
SLDA generates initial conditions for TDSLDA.

# Road to quantum turbulence

**Classical turbulence:** energy is transferred from large scales to small scales where it eventually dissipates.

**Kolmogorov spectrum:**  $E(k) = C \varepsilon^{2/3} k^{-5/3}$

$E$  – kinetic energy per unit mass associated with the scale  $1/k$   
 $\varepsilon$  - energy rate (per unit mass) transferred to the system at large scales.  
 $k$  - wave number (from Fourier transformation of the velocity field).  
 $C$  – dimensionless constant.



**Superfluid turbulence (quantum turbulence):** disordered set of quantized vortices. The friction between the superfluid and normal part of the fluid serves as a source of energy dissipation.

**Problem:** how the energy is dissipated in the superfluid system at small scales at  $T=0$ ? - „pure“ quantum turbulence

**Possibility:** vortex reconnections  $\rightarrow$  Kelvin waves  $\rightarrow$  phonon radiation

# Vortex reconnections

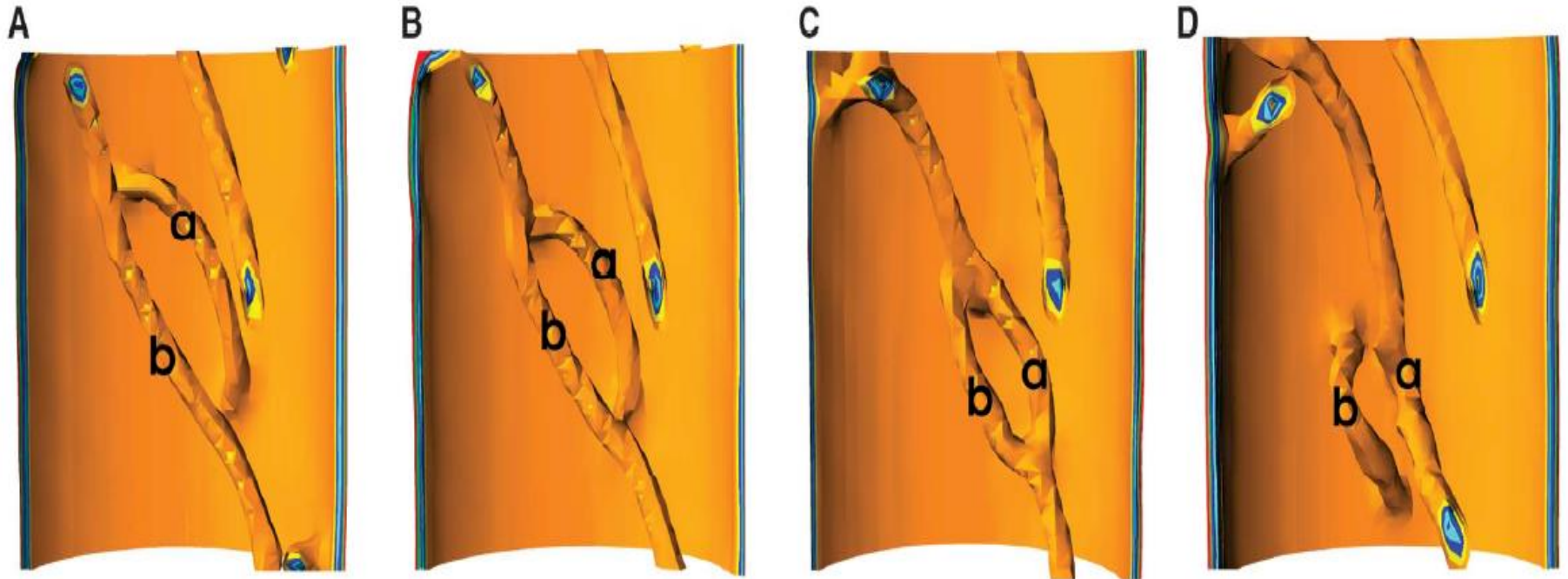
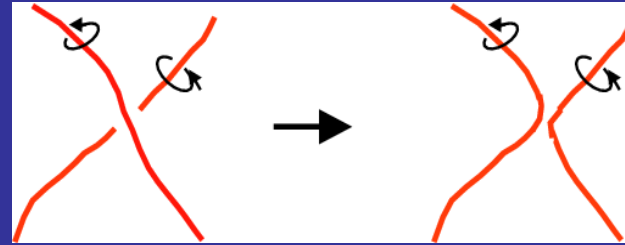
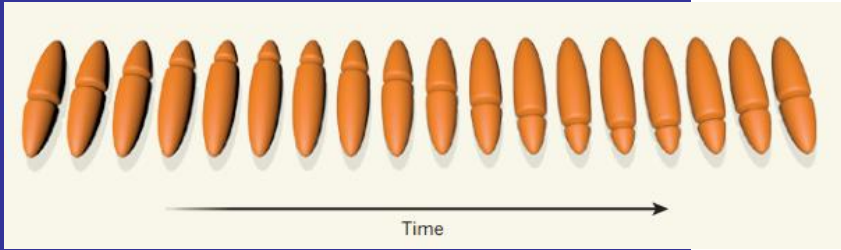


**Fig. 3. (A to D)** Two vortex lines approach each other, connect at two points, form a ring and exchange between them a portion of the vortex line, and subsequently separate. Segment (a), which initially belonged to the vortex line attached to the wall, is transferred to the long vortex line (b) after reconnection and vice versa.

# Soliton dynamics vs ring vortex – a controversy



MIT Experiment:  
Nature 499 (2013) 426

Theory prefers ring vortices:

A. Bulgac, et al.,  
Phys. Rev. Lett. 112, 025301 (2014)  
G. Wlazłowski, et al.  
Phys. Rev. Lett. (in press)

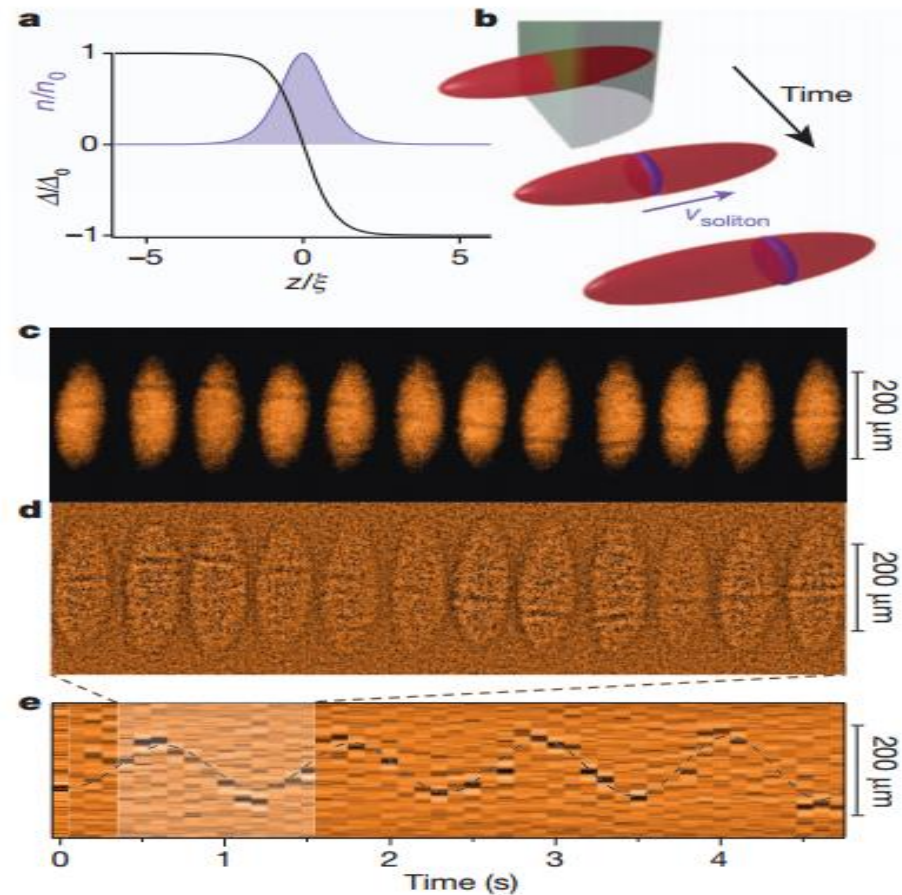


**Figure 1 | Creation and observation of solitons in a fermionic superfluid.** **a**, Superfluid pairing gap  $\Delta(z)$  for a stationary soliton, normalized by the bulk pairing gap  $\Delta_0$ , and density  $n(z)$  of the localized bosonic (fermionic) state versus position  $z$ , in the BEC (BCS) regime of the crossover, in units of the BEC healing length (BCS coherence length)  $\xi$ . **b**, Diagram of the experiment. A phase-imprinting laser beam twists the phase of one-half of the trapped superfluid by approximately  $\pi$ . The soliton generally moves at non-zero velocity  $v_{\text{soliton}}$ . **c**, Optical density and **d**, residuals (optical density minus a smoothed copy of the same image) of atom clouds at 815 G, imaged via the rapid ramp method<sup>34</sup>, showing solitons at various hold times after creation. One period of soliton oscillation is shown. The in-trap aspect ratio was  $\lambda = 6.5(1)$ . **e**, Radially integrated residuals as a function of time revealing long-lived soliton oscillations. The soliton period is  $T_s = 12(2)T_z$ , much longer than the trapping period of  $T_z = 93.76(5)$  ms, revealing an extreme enhancement of the soliton's relative effective mass,  $M^*/M$ .